C:N:P stoichiometry at the Bermuda Atlantic Time-series station in the North Atlantic Ocean

Arvind Singh[1, 2], Steven E. Baer[3], Ulf Riebesell[2], Adam C. Martiny[4], M. W. Lomas[1,3*]

[1]Bermuda Institute of Ocean Sciences, St. George's, GE01, Bermuda
[2]GEOMAR Helmholtz-Zentrum für Ozeanforschung Kiel, 24105 Kiel, Germany
[3]Bigelow Laboratory for Ocean Sciences, East Boothbay, ME 04544, USA
[4]University of California, Irvine, California 92697, USA.

*E–mail address of the corresponding author: mlomas@bigelow.org (M.W. Lomas)

Abstract

Nitrogen (N) and phosphorus (P) availability, in addition to other macro-and micronutrients, determine the strength of the ocean's carbon (C) uptake, and variation in the N:P ratio of inorganic nutrient pools is key to phytoplankton growth. A similarity between C:N:P ratios in the plankton biomass and deep-water nutrients was observed by Alfred C. Redfield around 80 years ago and suggested that biological processes in the surface ocean controlled deep ocean chemistry. Recent studies have emphasized the role of inorganic N:P ratios in governing biogeochemical processes, particularly the C:N:P ratio in suspended particulate organic matter (POM), with somewhat less attention given to exported POM and dissolved organic matter (DOM). Herein, we extend the discussion on ecosystem C:N:P stoichiometry but also examine temporal variation of stoichiometric relationships. We have analysed elemental stoichiometry in the suspended POM and total (POM + DOM) organic matter (TOM) pools in the upper 100 m, and in the exported POM and sub-euphotic zone (100 - 500 m) inorganic nutrient pools from the monthly data collected at the Bermuda Atlantic Time-series Study (BATS) site located in the western part of the North Atlantic Ocean. C:N and N:P ratios in the TOM were at least twice that in the POM, while C:P ratios were up to five times higher in the TOM compared to that in the POM. Observed C:N ratios in suspended POM were approximately equal to the canonical Redfield Ratio (C:N:P = 106:16:1), while N:P and C:P ratios in the same pool were more than twice the Redfield Ratio. Average N:P ratios in the subsurface inorganic nutrient pool were ~26:1, squarely between the suspended POM ratio and the Redfield Ratio. We have further linked variation in elemental stoichiometry with that of phytoplankton cell abundance observed at the BATS site. Findings from this study suggest that elemental ratios vary with depth in the euphotic zone mainly due to different growth rates of cyanobacterial cells. We have also

examined role of the Arctic Oscillation on temporal patterns in C:N:P stoichiometry. This study strengthens our understanding of the variability of elemental stoichiometry in different organic matter pools and should improve biogeochemical models by constraining the range of non-Redfield stoichiometry and the net relative flow of elements between pools.

Keywords: North Atlantic Ocean, BATS, Biogeochemistry, Phytoplankton, Stoichiometry

1. Introduction

Nitrogen (N) and phosphorus (P) are critical elements that control primary production in large portions of the surface ocean. Traditionally, N is considered a proximate and P is an ultimate limiting nutrient in surface waters (Tyrrell, 1999), but primary production in the North Atlantic Ocean has been suggested to be P stressed (Wu et al., 2000; Karl et al., 2001; Sañudo-Wilhelmy et al., 2001; Lomas et al., 2010). Alfred C. Redfield first noted the similarity between N:P ratios in surface ocean particulate organic matter (POM) and in deep-water inorganic nutrients; this observation was further extended to include carbon (Redfield, 1934). Oceanographic studies have consistently found mean plankton biomass to adhere to the Redfield Ratio (C:N:P = 106:16:1; Redfield, 1958; Copin-Montegut and Copin-Montegut, 1983; Geider and La Roche, 2002), and since then this ratio has become a fundamental tenet in marine biogeochemistry. Deviations from the canonical ratio have been used to provide insights into phytoplankton physiology (Goldman et al., 1979; Quigg et al., 2003), nutrient limitation of primary production (e.g., Falkowski and Raven, 1997; Moore et al., 2013), efficiency of biological carbon sequestration in the ocean (Sigman and Boyle, 2000) and the input/output balance of the marine N cycle (e.g., Gruber and Sarmiento, 1997). Geochemists use the Redfield conceptual model to determine the state of the marine N cycle using the N* proxy (e.g., Gruber and Sarmiento, 1997). In the context of this proxy, subsurface nutrient N:P ratios > 16:1 suggest net nitrogen gain, while ratios < 16:1 suggest net nitrogen loss (e.g., Gruber and Deutsch, 2014). However, this relatively simple point of view has been shown to yield up to four-fold overestimation of N_2 fixation rates when compared to directly measured rates (Mills and Arrigo, 2010). In part, this overestimation is due to the production and sedimentation of non-N_2 fixer biomass that can occur at ratios much greater than Redfield, particularly in the subtropical and

85 tropical oceans (Singh et al., 2013; Martiny et al., 2013; Teng et al., 2014). Furthermore, an
86 ocean circulation model has shown that the N:P ratio of biological nutrient removal varies
87 geographically, from 12:1 in the polar ocean to 20:1 in the sub–Antarctic zone, regions where N_2
88 fixation is not thought to be important (Weber and Deutsch, 2010). With a better understanding
89 of N cycle processes, the validity of the Redfield model for nutrient uptake has been questioned
90 (Sañudo-Wilhelmy et al., 2004; Mills and Arrigo, 2010; Zamora et al., 2010).

91 Biologically speaking, a fixed N:P ratio, like the Redfield Ratio, would suggest that
92 nutrients are taken up in that ratio during production of new organic matter (Redfield, 1958;
93 Lenton and Watson, 2000). This conceptual model has been challenged by the fact that the
94 variability in nutrient requirements is related to the functioning and evolution of microbes
95 (Arrigo, 2005). The N:P ratio in phytoplankton need not be in the canonical ratio and can vary
96 widely from coastal upwelling to transitional to oligotrophic regions of the ocean. The observed
97 ratio varies with taxa and growth conditions (Arrigo et al., 1999; Quigg et al., 2003; Klausmeier
98 et al., 2004). For example, it has been shown that non–Redfield nutrient utilization is common
99 during blooms (Arrigo et al., 1999) and in regions dominated by cyanobacteria (Martiny et al.,
100 2013). The N:P ratio of *Synechococcus* and *Prochlorococcus*, small and abundant phytoplankton
101 cells in the open ocean, varies from 13.3 to 33.2 and 15.9 to 24.4, respectively, during
102 exponential growth, while the ratio can be as high as 100 during PO_4^{3-} limited growth (Bertilsson
103 et al., 2003; (Heldal et al., 2003). Another cyanobacteria, the N_2 fixer *Trichodesmium* has an
104 N:P ratio that varies from 42 to 125 (Karl et al., 1992), while in general diatoms have a ratio of
105 ~11:1 (Quigg et al., 2003; Letelier and Karl, 1996; Mahaffey et al., 2005). Excess downward
106 dissolved organic nitrogen (DON) fluxes relative to NO_3^- are associated with *Trichodesmium*

abundance (Vidal et al., 1999). Thus the relative abundance of different phytoplankton functional groups may lead to coupling of N and P cycles in non-Redfieldian proportions.

Considerable effort has been made to understand the variability and controls on the N:P ratio in the dissolved inorganic nutrient pool (e.g., Gruber and Sarmiento, 1997; Pahlow and Riebesell, 2000; Arrigo, 2005). In contrast, analysis of C:N:P ratios in particulate organic matter (POM) and dissolved organic matter (DOM) are more scarce (Karl et al., 2001; Letscher et al., 2013). The C:N:P ratio however, has great relevance in oceanography, as it connects the 'currency' of the ocean, i.e., carbon, to some of its controlling variables, N and P. Here, we present a detailed analysis of C:N:P stoichiometry of POM and TOM along with N:P stoichiometry of dissolved inorganic nutrients at the Bermuda Atlantic Time-series Study (BATS) for an eight year period. The observed ratios are correlated with and discussed in the context of co-measured biological parameters such as cell abundances of different phytoplankton groups and chlorophyll *a*. The goal of this study was to quantitatively assess C:N:P ratios in all (POM, TOM and inorganic nutrients) the pools and their deviations from the Redfield Ratio, and relationships to biogeochemical cycling.

2. Methods

2.1 Data Availability

Since 1988, the BATS site, located in the western subtropical North Atlantic Ocean (31° 40'N, 64° 10'W), has provided a relatively unique time–series record of nutrient biogeochemical cycles. However, data on total organic C (TOC), total organic N (TON) and total organic P (TOP) and particulate organic C (POC), particulate organic N (PON), and particulate organic P (POP) have only been collected concurrently since 2004. These data were collected from seven

130 different depths (5, 10, 20, 40, 60, 80 and 100 m) over the euphotic zone. We obtained these data
131 from the BATS website (bats.bios.edu) and analysed the data record from 2004-2012.
132
133 **2.2 Analytical Methods**
134 Samples for nitrate (NO_3^-) and phosphate (PO_4^{3-}) were gravity filtered (0.8 μm) and
135 frozen (-20°C) in HDPE bottles until analysis (Dore et al., 1996). NO_3^- and PO_4^{3-} were measured
136 using a Technicon autoanalyser with an estimated inaccuracy of ~0.12 μmol kg^{-1} and 0.02 μmol
137 kg^{-1}, respectively (Bates and Hansell, 2004). The Magnesium Induced Co-precipitation
138 (MAGIC) soluble reactive P (SRP) method (Karl and Tein, 1997) was used starting in late 2004
139 to improve both the sensitivity and the accuracy of the inorganic PO_4^{3-} analysis (Lomas et al.,
140 2010). POC and PON samples were filtered on pre-combusted (450° C, 4h) Whatman GF/F
141 filters (nominal pore size 0.7 μm) and frozen (-20°C) until analysis on a Control Equipment 240-
142 XA or 440-XA elemental analyzer (Steinberg et al., 2001; Lomas et al., 2013). POP was
143 analyzed using the ash-hydrolysis method with oxidation efficiency and standard recovery
144 checks (Lomas et al., 2010). TOC and TON concentrations were determined using high
145 temperature combustion techniques (Carlson et al., 2010). Total P (TP) concentrations were
146 quantified using a high temperature/persulfate oxidation technique and TOP calculated by
147 subtraction of the MAGIC-SRP value (Lomas et al., 2010). Ideally DOM concentrations would
148 have been estimated by subtracting POM from its total organic concentrations, e.g., [DOC] =
149 [TOC] - [POC], but we did not have paired TOC (and TON) and POC (and PON) values;
150 corresponding POC (and PON) values were taken at slightly different depths but on the same
151 sampling day. Nevertheless, subtraction would not have had a substantial impact because, on
152 average, POC and PON values in the upper 100 m were <4% of TOC and TON, respectively

153 (Fig. 1). Both the accuracy and precision of dissolved organic compound concentrations decrease
154 with depth as concentrations of inorganic nutrients increase to dominate the total pools.

155 Chlorophyll *a* pigments were analyzed by HPLC using the method of van Heukelem and
156 Thomas (2001). Samples for flow cytometric enumeration of pico- and nano-plankton were
157 collected on each cruise and analysed as described in Lomas et al. (2013). Export fluxes of POC,
158 PON and POP were estimated using surface-tethered particle interceptor traps deployed at 200 m
159 depth as described in previous publications (Lomas et al., 2010; Steinberg et al., 2001).
160 Elemental masses of material captured in sediment traps, trap collection surface area and
161 deployment length were used to calculate fluxes (see Lomas et al., 2013 for a more detailed
162 methodology on all the described parameters in the method section).

163

164 **2.3 Data Processing**

165 Our POM and TOM analysis was restricted to the upper 100 m, which also reflects the
166 approximate mean depth of the euphotic zone at BATS (Siegel et al., 2001) and the zone where
167 nutrients are depleted to near analytical detection. All data presented as elemental ratios are in
168 mol/mol units. Mixed layer depth was defined as a 0.125 kg m^{-3} difference in seawater density
169 from the surface (Gardner et al., 1995). While mixed layer depths (MLD) were always deepest
170 during winter, the exact timing of the deepest mixing shifted between years. For example, during
171 2005, the MLD was deepest in March, while it was deepest during February in 2006. Therefore,
172 when presenting data on an annual cycle, we aligned our data to the measured timing of deep
173 mixing in each year and combined all the data to a single 12 month composite (e.g., Carlson et
174 al., 2009). Generally the mixed layer depth was no deeper than ~25m in summer, thus we used

this depth range, 0-25m, to represent the 'surface' data and present our analysis in two depth bin, 0-25m and 25-100m.

3. Results

We present time-series data of chemical constitutes in POM and TOM pools (Fig. 1). We further calculated depth-averaged ratios of the chemical constitutes. We first calculated average concentration of each element over the depth segment (e.g., 0-25 m) and then calculated the ratios based upon those averages. Over the entire length of the time-series, euphotic zone TON:TOP ratios varied between 34 and 130 (Fig. 2a), while TOC:TOP ratios varied between 450 and 1952 (Fig. 2b), and TOC:TON varied between 11 and 17 (Fig. 2c).

Suspended euphotic zone PON:POP ratios were generally lower than TON:TOP ratios (Fig. 2, Table 1). The PON:POP ratio ranged from 7 to 140. Similarly POC:POP ratios were much lower than TOC:TOP, varying from 45 to 532. The POC:PON ratio ranged between 1 and 19. Elemental ratios in the TOM and POM were significantly greater than the Redfield Ratio ($p < 0.05$; z test) with the exception of the POC:PON ratio.

3.1. Annual patterns

3.1.1 Concentrations of POM and TOM

There were annual oscillations in POM pools in the upper 100 m (Fig. 1). TOC also showed annual oscillations, however, TON concentrations were relatively constant throughout the study period. The pattern of TOP was an increasing trend during early 2007 until early 2008 (TOP = 0.0936 × decimal year - 187.8; $r^2 = 0.77$, $p < 0.05$). However, there were no long term sustained changes in concentration of POM and TOM.

198

199 **3.1.2 C:N:P ratios in POM and TOM**

200 There were no discernible year-over-year trends in the POM stoichiometry (Fig. 2).
201 Amplitude of variation in the C:N:P ratios of POM was less than that in TOM. TON:TOP and
202 TOC:TOP ratios showed a decreasing trend throughout the year 2007 (r^2 = 0.46, p < 0.05),
203 which was due to an increasing trend in TOP concentration in that year (Fig. 1). There was no
204 annual trend in the TOC:TON ratio. Overall, like POM and TOM concentration patterns, there
205 were no long-term sustained changes in TOC:N:P ratios.

206

207 **3.2 Seasonal variations**

208 **3.2.1 Concentrations of POM and TOM**

209 There was greater variability in C and N pools in the 0-25 m range compared to that in
210 the 25-100 m range (Figs. 4 and 5). In the 0-25 m depth range, TOC showed an increasing trend
211 after deep mixing during the following five months before reaching a plateau (~67 μmol kg^{-1}).
212 POC increased in the first month after deep mixing and then decreased during the next two
213 months and remained constant (~2 μmol kg^{-1}) for the rest of the year (Fig. 4a). The pattern in
214 PON was similar to POC, while those in TON and TOC were opposite to each other during the
215 first two months after mixing and then increased until the sixth month (Fig. 4a, b). These higher
216 values of TOC and TON (observed in both 0-25 m and 25-100 m depth segments) in the sixth
217 month might be attributed to the higher occurrence of *Trichodesmium* colonies during August at
218 BATS (Orcutt et al., 2001; Singh et al., 2013). TOP and POP increased during and one month
219 after the deep mixing in the 0-25m depth range (Figs. 4c). Some of these trends (e.g., higher

220 values of TOC and TON in the sixth month) were also apparent in the 25-100 m depth range but
221 were not as prominent as in the 0-25 m depth range (Figs. 4 and 5).
222
223 **3.2.2 C:N:P ratios in POM and TOM**
224 TON:TOP (68 ± 9) and PON:POP (36 ± 11) values were greater than the Redfield Ratio
225 ($p < 0.05$) (Table 1). Patterns in TOC:TOP and TON:TOP ratio, and POC:POP and PON:POP
226 were similar to each other (Fig. 6a, b). TOC:TOP (983 ± 168) and POC:POP (210 ± 67) values
227 were much higher than the Redfield Ratio of 106 ($p < 0.05$). TOC:TON (15 ± 0.5) increased for
228 the two months following deep mixing and decreased until the seventh month (Fig. 6c).
229 POC:PON (6 ± 3) increased in the next month after deep mixing, but remained around the
230 Redfield Ratio throughout the year. Minimal variability in concentration and ratios in the 25-100
231 m depth range suggests confinement of the more dynamic biogeochemical processes to within
232 the mixed layer, i.e. within 0-25 m (Figs. 5 and 7).
233
234 **3.2.3 N:P ratios in inorganic nutrients**
235 The average NO_3^-:PO_4^{3-} ratio was 25.6 ± 9.1 in the 100-500 m depth range at BATS,
236 which is greater than the Redfield Ratio (Table 1). We excluded data from the top 100 m in this
237 analysis due to low precision relative to the mean nutrient values which are at or near analytical
238 detection limits due to active biological uptake. NO_3^- and PO_4^{3-} were at their highest
239 concentrations before deep mixing and decreased immediately following the month of deepest
240 mixing and remained constant for the rest of the year (Fig. 8). The decrease in NO_3^- and PO_4^{3-}
241 concentrations was likely due to dilution with low nutrient surface water during mixing.
242

3.2.4 N:P ratios in the particulate flux at 200 m

The PON fluxes increased during and peaked immediately after winter mixing, while POP fluxes showed elevated values before and shortly after the time of deep mixing (Fig. 8). The N:P ratio of export fluxes was nearly twice that of PON:POP ratio in the suspended matter (upper 100 m; Table 1).

3.2.5 Chlorophyll *a* and phytoplankton cell abundance

Chlorophyll *a* values decreased after the spring bloom that was stimulated by deep mixing (Fig. 9a). *Prochlorococcus* was dominant during the oligotrophic period of the year, while these were least abundant around the time of deep mixing (Fig. 9b). In contrast, *Synechococcus* and picoeukaryotes were more abundant during the more productive season (Fig. 9c,d), and followed the annual pattern in Chlorophyll *a*. There was no discernible seasonal pattern in nanoeukaryote abundance (Fig. 9e).

4. Discussion

From the approximately eight years of BATS data presented here, it is apparent that the total and particulate organic matter C:N:P stoichiometries are not a long-term fixed ecosystem property, but vary seasonally and deviate substantially from the canonical Redfield Ratio. Observed C:N:P ratios in TOM and POM were much greater than the Redfield Ratio, averaging 983:68:1 and 210:36:1, respectively, for the entire dataset (Figs. 2, 4, 5).

4.1 Connections among POM, TOM and inorganic nutrients

Redfield hypothesized what was effectively a two-box model of nutrients shuttling between particulate and dissolved form. However, there are number of different biological, chemical and physical processes acting on particles as they settle through the water column. Higher N:P ratios in the particulate fluxes than in the suspended matter could be due to the preferential export of N or preferential remineralisation of P, but similar C:N ratios in the fluxes and suspended matter would lend more support to the latter scenario (Figs. 4, 8; Table 1; Monteiro and Follows, 2012). The N:P ratio of export fluxes was also generally more than twice that of the dissolved NO_3^-:PO_4^{3-} ratio at depth (Fig. 8c). The preferential remineralization of P from settling material could potentially explain this difference, as there is little evidence for N loss in this well-oxygenated region, however the advective flux of low NO_3^-:PO_4^{3-} waters needs to be considered. Indeed, the literature indicates that sub-euphotic waters at BATS are a mixture of water originated at the north of the site, which has characteristically low NO_3^-:PO_4^{3-} ratios (Bates and Hansell, 2004; Singh et al., 2013). The processes of remineralization are not direct from particulate to inorganic pools and indeed, cycling through the dissolved organic pool, which dominates TOM, is important. One explanation for the TON:TOP ratio being greater than the Redfield Ratio is that TON is less reactive than TOP and broken down mainly in the subsurface layer (Letscher et al., 2013), while TOP is labile or semi-labile and both remineralized and assimilated at a shallower depth (Björkman et al., 2000). Consequently, TOP has faster turnover times (Clark et al., 1998). In contrast to this interpretation, our observations suggest that TON and TOP values increase slightly with depth suggesting a net (i.e., remineralization exceeding assimilation) flow of material from the particulate organic pool to the dissolved organic pool for both elements (comparing data in Figs. 4 and 5).

Our results on the TON:TOP ratio have important implications in ocean biogeochemistry of oligotrophic waters where DON and DOP concentrations in the sunlit layers exceed the concentration of inorganic nutrients by an order of magnitude. Dissolved organic pools are essential in sustaining phytoplankton growth in these regions (Church et al., 2002; Williams and Follows, 1998). Nutrient levels decide phytoplankton growth and their stoichiometry (Klausmeier et al., 2004), hence TON:TOP in the oligotrophic regions might determine optimal N:P stoichiometry of phytoplankton rather than the inorganic pools alone.

4.2 Linkages of concentrations and ratios of POM and TOM to chlorophyll *a* and phytoplankton

We hypothesize that C:N:P ratios in the aggregated phytoplankton community itself changes the elemental stoichiometry of the POM and TOM pools. The C:N:P ratio is different in different phytoplankton communities and their biological uptake and degradation could potentially change the elemental stoichiometry of the particulate and dissolved organic matter. The C:N:P ratio varies geographically and its pattern correlates with global variations in temperature, overall nutrient concentrations and phytoplankton functional groups. These latitudinal patterns in the C:N:P ratio have been attributed to changes in phytoplankton community as polar (colder) regions have a high abundance of diatoms with low N:P and C:P ratios, in contrast to the directly measured high elemental ratios in cyanobacteria from warmer regions (Martiny et al., 2013). So how and why does C:N:P ratio vary in phytoplankton communities? Two mechanisms could explain variability in the C:N:P ratios in a phytoplankton community. The first mechanism suggests that the taxonomic composition of a phytoplankton community influences its elemental composition. Elemental ratios inside a cell are controlled by

310 growth strategies (Klausmeier et al., 2004) . Studies have reported low C:P and N:P ratios in fast
311 growing diatoms (e.g., Price, 2005), whereas slower growing cyanobacteria have C:P and N:P
312 ratios higher than the Redfield Ratio (Bertilsson et al., 2003; Martiny et al., 2013). More
313 precisely, it is not so much the growth rate that determines the difference, but the machinery
314 invested in nutrient acquisition versus protein production.

315 The second mechanism links the nutrient supply ratio to a taxonomically 'hard-wired'
316 cellular elemental ratio (Rhee, 1978). Chlorophyll *a* values were anti-correlated with TOC
317 values ($r^2 = 0.76$, $p < 0.05$). The gradual increase in Chlorophyll *a* during the four months before
318 deep mixing is due to similar increase in MLD before deep mixing (Fig. 3), which suggests that
319 there may be enhanced nutrient flux into the upper layer well before deep mixing (e.g., Fawcett
320 et al. 2014). *Prochlorococcus* and *Synechococcus* profiles were correlated to each other in the
321 first seven months from the point of deepest mixing ($r^2 = 0.58$, $p < 0.05$) and there was no
322 relation in the rest of the year in the 0-25 m depth range. Furthermore, *Synechococcus* cell
323 abundance was correlated with POC ($r^2 = 0.67$ $p < 0.05$), PON ($r^2 = 0.47$ $p < 0.05$), POP ($r^2 =$
324 0.29 $p < 0.05$) and anti-correlated with TOC values ($r^2 = 0.72$ $p < 0.05$) in the 0-25 m depth
325 range. *Synechococcus* is more abundant during the more productive season whereas
326 *Prochlorococcus* is dominant during the highly oligotrophic part of the year. Such patterns are
327 typically observed in many parts of the ocean. The seasonal pattern of picoeukaryote abundance
328 was similar to that of *Synechococcus* ($r^2 = 0.58$ $p < 0.05$) and Chlorophyll *a* ($r^2 = 0.81$ $p < 0.05$).
329 POC:PON:POP ratios in *Prochlorococcus*, *Synechococcus* and picoeukaryote are 234:33:1,
330 181:33:1 and 118:15:1, respectively at the BATS site (Martiny et al., 2013 and Lomas et al.,
331 unpublished data), which clearly suggests imprints of a mixture of *Prochlorococcus*,
332 *Synechococcus* on the observed POM stoichiometry presented in Table 1. Biomass of

333 *Prochlorococcus*, *Synechococcus* and picoeukaryotes together contributes ~40% to the POC pool
334 (Casey et al. 2013) and ~75% to the PON pool (Fawcett et al. 2011), with major contributions
335 from each group varying seasonally. Hence, variability in biological parameters could potentially
336 explain a significant fraction of the variability in the POM and TOM ratios, but not all of it. So
337 what else drives the variability in the C:N:P ratios?

338 We analysed trends in the TON:TOP and TOC:TOP ratios for December 2006 to January
339 2008 data along with phytoplankton cell abundances for the top 100 m BATS data. Since the
340 variation in TON:TOP and TOC:TOP were due to an increasing trend in TOP, we correlated
341 TOP concentrations with a lag of three months (there is a time lag between phytoplankton and
342 elemental abundance as observed by Singh et al., 2013) in phytoplankton cell abundances (data
343 during September 2006 to November 2007; Fig. 10a). We observed significant anti-correlation
344 ($r^2 = 0.61$, $p < 0.001$) between nanoeukaryotes and TOP but the data did not correlate with other
345 phytoplankton groups (Fig. 10a). In the paucity of elemental composition data on
346 nanoeukaryotes, we hypothesize that these cells have a high requirement for P and are potentially
347 meeting that requirement by assimilating TOP.

348 We further analysed this increasing trend in the TOP concentration with climate indices.
349 The Arctic Oscillation is a major climatic phenomenon in the North Atlantic Ocean (Thompson
350 and Wallace, 1999). Positive trends in the Arctic Oscillation lead to higher temperatures,
351 advanced spring, and increased CO_2. This could lead to enhanced uptake of CO_2 during spring as
352 has been found in terrestrial systems (Schaefer et al., 2005). Higher build-up of organic matter
353 would require more P and hence we correlated TOP concentration with monthly Arctic
354 Oscillation index with a lag of a year (monthly Arctic Oscillation indices are from November
355 2005 to December 2006, because there is a lag of one year before climatic oscillations in the

North Atlantic show its impact on surface biogeochemistry; Fromentin and Planque, 1996). We observed a significant correlation ($r^2 = 0.46$, $p < 0.01$) between the Arctic Oscillation and TOP concentrations (Fig. 10b). Since variations in phytoplankton cell abundances and climate variability could not explain all the variation in the elemental stoichiometry, other mechanisms are yet to be identified to explain the observed variability in the elemental stoichiometry.

4.3 Role of DOM in microbial carbon export

Many biogeochemical model estimates of export production assume Redfield stoichiometry in export fluxes but a non-Redfieldian approach has gained appreciation recently (Letscher and Moore, 2015). Export production is estimated to be 3-4 mol C m^{-2} yr^{-1} in the BATS region (Jenkins, 1982; Emerson, 2014), which requires more nutrient input than observations suggest (Williams and Follows, 1998). A possible mechanism to sustain such export production is the supply of DOM to the sunlit layer.

DOM consists of complex compounds whose chemical characterization is incomplete, but it is evident that DOM elemental stoichiometry differs drastically from the Redfield Ratio. Differential production and degradation of DON and DOP with lifetimes comparable to the gyre circulation could potentially change the overall stoichiometry of nutrient supply (Voss and Hietanen, 2013). Preferential degradation of DOP rather than DON expands the niche of diazotrophs beyond that created by subsurface denitrification. Diazotrophs can quickly utilize recycled DOP (Dyhrman et al., 2006). Simultaneously, these diazotrophs release DON (Mulholland, 2007), which can be used by other phytoplankton, but this DON likely has associated DOP. In the P stressed Sargasso Sea, DOP contributes up to 50% of P demand for primary production (Lomas et al. 2010) and up to 70% to the exported POP (Roussenov et al.,

2006; Torres-Valdés et al., 2009). Indeed, a 1-D biogeochemical model for BATS that included an explicit DOP pool and a generic DOM pool significantly improved the capture of natural variability in both particulate (suspended and exported) and dissolved (organic and inorganic) pools (Salihoglu et al. 2007). These model results, as well as others connecting DOP cycling to particulate P export (e.g., Roussenov et al. 2007), suggest a strong need for direct rate measurements of DOM production and assimilation (e.g., Mahaffey et al. 2014).

Conclusion

Our time-series analysis suggests temporal and depth variability in the C:N:P ratio in the Sargasso Sea. C:N:P ratios in the TOM were significantly higher than the canonical Redfield Ratio, while C:N was similar to the Redfield Ratio in the POM. We observed seasonal variability in stoichiometry but on average the TOC:TON:TOP ratio was 983:68:1 and the POC:PON:POP was 210:36:1. Seasonal variation in POM stoichiometry appears to be largely driven by the growth of *Synechococcus* during winter mixing, while flourishing of *Prochlorococcus* cells during the oligotrophic period (fall) could also explain some variability in the stoichiometry. The C:N:P ratio in *Prochlorococcus* cells resembles observed mean POC:PON:POP ratio at BATS (210:36:1). The N:P ratio in subsurface inorganic nutrients was also greater (N:P = 26) than the Redfield Ratio in this region. We observed a significant decreasing trend in TON:TOP and TOC:TOP during 2007, which was due to an increase in TOP concentration and could have been partly driven by the Arctic Oscillation and a decrease in the relative abundance of nanoeukaryotes. Other causes for the observed variations in the elemental stoichiometry need to be explored; however, this elemental stoichiometry analysis may improve biogeochemical models, which have hitherto assumed Redfield stoichiometry to estimate export fluxes.

402

403

404

Acknowledgments

We sincerely thank the research technicians, captains and crew of BATS cruises for their contribution to the data, and the National Science Foundation Chemical and Biological Oceanography Programs for continued support of the BATS program through the following awards: OCE 88–01089, OCE 93–01950, OCE 9617795, OCE 0326885, OCE 0752366, and OCE-0801991. This work was financially supported by Centre of Excellence (CofE) funded by Nippon Foundation (NF)–Partnership for Observations of the Global Ocean (POGO) and a grant (CP1213) of the Cluster of Excellence 80 'The Future Ocean' to AS.

References

Arrigo, K. R.: Marine microorganisms and global nutrient cycles, Nature, 437, 349–355, doi:10.1038/nature04158, 2005.

Arrigo, K. R., Robinson, D. H., Worthen, D. L., Dunbar, R. B., DiTullio, G. R., VanWoert, M. and Lizotte, M. P.: Phytoplankton Community Structure and the Drawdown of Nutrients and CO_2 in the Southern Ocean, Science, 283, 365–367, doi:10.1126/science.283.5400.365, 1999.

Bates, N. R. and Hansell, D. A.: Temporal variability of excess nitrate in the subtropical mode water of the North Atlantic Ocean, Mar. Chem., 84, 225–241, doi:10.1016/j.marchem.2003.08.003, 2004.

Bertilsson, S., Berglund, O., Karl, D. M. and Chisholm, S. W.: Elemental composition of marine *Prochlorococcus* and *Synechococcus*: Implications for the ecological stoichiometry of the sea, Limnol. Oceanogr., 48(5), 1721–1731, 2003.

Björkman, K., Thomson-Bulldis, A. L. and Karl, D. M.: Phosphorus dynamics in the North Pacific subtropical gyre, Aquat. Microb. Ecol., 22, 185–198, 2000.

Carlson, C. A., Morris, R., Parsons, R., Treusch, A. H., Giovannoni, S. J. and Vergin, K.: Seasonal dynamics of SAR11 populations in the euphotic and mesopelagic zones of the northwestern Sargasso Sea, ISME J., 3(3), 283–295, 2009.

Carlson, C. A., Hansell, D. A., Nelson, N. B., Siegel, D. A., Smethie, W. M., Khatiwala, S., Meyers, M. M. and Halewood, E.: Dissolved organic carbon export and subsequent remineralization in the mesopelagic and bathypelagic realms of the North Atlantic basin, Deep-Sea Res. II, 57, 1433–1445, doi:10.1016/j.dsr2.2010.02.013, 2010.

Casey, J.R., Aucan, J.P., Goldberg, S.R., Lomas, M.W. 2013. Changes in partitioning of carbon amongst photosynthetic pico- and nano-plankton groups in the Sargasso Sea in response to changes in the North Atlantic Oscillation. Deep Sea Res. II, 93:58-70.

Church, M. J., Ducklow, H. W. and Karl, D. M.: Multiyear increases in dissolved organic matter inventories at Station ALOHA in the North Pacific Subtropical Gyre, Limnol. Oceanogr., 47(1), 1–10, 2002.

Clark, L. L., Ingall, E. D. and Benner, R.: Marine phosphorus is selectively remineralized, Nature, 393(6684), 426, doi:10.1038/30881, 1998.

Copin-Montegut, C. and Copin-Montegut, G.: Stoichiometry of carbon, nitrogen, and phosphorus in marine particulate matter, Deep-Sea Res. II, 30(1), 31–46, 1983.

Dore, J. E., Houlihan, T., Hebel, D. V., Tien, G. A., Tupas, L. M. and Karl, D. M.: Freezing as a method of sample preservation for the analysis of dissolved inorganic nutrients in seawater, Mar. Chem., 53, 173–185, 1996.

Dyhrman, S. T., Chappel, P. D., Haley, S. T., Moffet, J. W., Orchard, E. D., Waterbury, J. B. and Webb, J. B.: Phosphonate utilization by the globally important marine diazotroph *Trichodesmium*, Nature, 439, 68–71, doi:10.1038/nature04203, 2006.

Emerson, S.: Annual net community production and the biological carbon flux in the ocean, Glob. Biogeochem. Cycles, 28, 14–28, doi:10.1002/2013GB004680, 2014.

Falkowski, P. G. and Raven, J. A.: Aquatic photosynthesis, Blackwell Science, Oxford, UK., 1997.

Fawcett, S.E., Lomas, M.W., Casey, J.R., Ward, B.B., Sigman, D.M. 2011. Assimilation of upwelled nitrate by small eukaryotes in the Sargasso Sea. Nature Geoscience, 4:717-722.

Fawcett, S.E., Lomas, M.W., Ward, B.B., Sigman, D.M. 2014. The counterintuitive effect of summer-to-fall mixed layer deepening on eukaryotic new production in the Sargasso Sea. Glob. Biogeochem. Cycles, 10.1002/2013GB004579.

Fromentin, J.-M. and Planque, B.: Calanus and environment in the eastern North Atlantic. II. Influence of the North Atlantic Oscillation on C. finmarchicus and C. helgolandicus, Mar. Ecol. Prog. Ser., 134, 111–118, 1996.

Gardner, W. D., Chung, S. P., Richardson, M. J. and Walsh, I. D.: The oceanic mixed-layer pump, Deep-Sea Res. II, 42(2-3), 757–775, 1995.

Geider, R. J. and La Roche, J.: Redfield revisited: variability of C:N:P in marine microalgae and its biochemical basis, Eur. J. Phycol., 37, 1–17, doi:10.1017/S0967026201003456, 2002.

Goldman, J. C., McCarthy, J. J. and Peavey, D. G.: Growth rate influence on the chemical composition of phytoplankton in oceanic waters, Nature, 279, 210–215, 1979.

Gruber, N. and Deutsch, C. A.: Redfield's evolving legacy, Nat. Geosci., 7(12), 853–855, 2014.

Gruber, N. and Sarmiento, J. L.: Global patterns of marine nitrogen fixation and Denitrification, Glob. Biogeochem. Cycles, 11(2), 235–266, 1997.

Heldal, M., Scanlal, D. J., Norland, S., Thingstad, F. and Mann, N. H.: Elemental composition of single cells of various strains of marine *Prochlorococcus* and *Synechococcus* using X-ray microanalysis, Limnol. Oceanogr., 48(5), 1732–1743, 2003.

Heukelem, L. V. and Thoams, C. S.: Computer-assisted high-performance liquid chromatography method development with applications to the isolation and analysis of phytoplankton pigments, J. Chromatogr. A, 910, 31–49, 2001.

Jenkins, W. J.: Oxygen utilization rates in the North Atlantic subtropical gyre and primary production in oligotrophic systems, Nature, 300(5889), 246–248, 1982.

Karl, D. M. and Tein, G.: Temporal variability in dissolved phosphorus concentrations in the subtropical North Pacific Ocean, Mar. Chem., 56, 77–96, 1997.

Karl, D. M., Letelier, R., Hebel, D. V., Bird, D. F. and Winn, C. D.: *Trichodesmium* blooms and new nitrogen in the north Pacific gyre, in Marine Pelagic Cyanobacteria: *Trichodesmium* and other Diazotrophs, pp. 219–237, Springer, Netherlands., 1992.

Karl, D. M., Björkman, K. M., Dore, J. E., Fujieki, L., Hebel, D. V., Houlihan, T., Letelier, R. M. and Tupas, L. M.: Ecological nitrogen-to-phosphorus stoichiometry at station ALOHA, Deep-Sea Res. II, 48, 1529–1566, 2001.

Klausmeier, C. A., Litchman, E., Daufresne, T. and Levin, S. A.: Optimal nitrogen-to-phosphorus stoichiometry of phytoplankton, Nature, 429, 171–174, 2004.

Lenton, T. M. and Watson, A. J.: Redfield revisited 1. Regulation of nitrate, phosphate, and oxygen in the ocean, Glob. Biogeochem. Cycles, 14(1), 225–248, 2000.

Letelier, R. M. and Karl, D. M.: Role of *Trichodesmium* spp. in the productivity of the subtropical North Pacific Ocean, Mar. Ecol. Prog. Ser., 133, 263–273, 1996.

Letscher, R. T. and Moore, J. K.: Preferential remineralization of dissolved organic phosphorus and non-Redfield DOM dynamics in the global ocean: Impacts on marine productivity, nitrogen fixation, and carbon export, Glob. Biogeochem. Cycles, 29(3), 325–340, doi:10.1002/2014GB004904, 2015.

Letscher, R. T., Hansell, D. A., Carlson, C. A., Lumpkin, R. and Knapp, A. N.: Dissolved organic nitrogen in the global surface ocean: Distribution and fate, Glob. Biogeochem. Cycles, 27, 1–13, doi:10.1029/2012GB004449, 2013.

Lomas, M. W., Burke, A. L., Lomas, D. A., Bell, D. W., Shen, C., Dyhrman, S. T. and Ammerman, J. W.: Sargasso Sea phosphorus biogeochemistry: an important role for dissolved organic phosphorus (DOP), Biogeosciences, 7, 695–710, 2010.

Lomas, M. W., Bates, N. R., Johnson, R. J., Knap, A. H., Steinberg, D. K. and Carlson, C. A.: Two decades and counting: 24-years of sustained open ocean biogeochemical measurements in the Sargasso Sea, Deep-Sea Res. II, 93, 16–32, 2013.

Mahaffey, C., Michaels, A. F. and Capone, D. G.: The conundrum of marine nitrogen fixation, Am. J. Sci., 305, 546–595, 2005.

Mahaffey, C., Reynolds, S., Davis, C. E., and Lohan, M. C. 2014. Alkaline phosphatase activity in the subtropical ocean: insights from nutrient, dust and trace metal addition experiments. Front. Mar. Sci. 1:73. doi: 10.3389/fmars.2014.00073

Martiny, A. C., Pham, C. T. A., Primeau, F. W., Vrugt, J. A., Moore, J. K., Levin, S. A. and Lomas, M. W.: Strong latitudinal patterns in the elemental ratios of marine plankton and organic matter, Nat. Geosci., 6, 279–283, doi:10.1038/NGEO1757, 2013.

Mills, M. M. and Arrigo, K. R.: Magnitude of oceanic nitrogen fixation influenced by the nutrient uptake ratio of phytoplankton, Nat. Geosci., 3, 412–416, doi:10.1038/NGEO856, 2010.

Monteiro, F. M. and Follows, M. J.: On nitrogen fixation and preferential remineralization of phosphorus, Geophys. Res. Lett., 39, L06607, doi:10.1029/2012GL050897, 2012.

Moore, C. M., Mills, M. M., Arrigo, K. R., Berman-Frank, I., Bopp, L., Boyd, P. W., Galbraith, E. D., Guieu, C., Jaccard, S. L., Jickells, T. D., La Roche, J., Lenton, T. M., Mahowald, N., Marañón, E., Marinov, I., Moore, J. K., Nakatsuka, T., Oschlies, A., Saito, M. A., Thingstad, T. F., Tsuda, A. and Ulloa, A.: Processes and patterns of oceanic nutrient limitation, Nat. Geosci., 6, 701–710, doi:10.1038/NGEO1765, 2013.

Mulholland, M. R.: The fate of nitrogen fixed by diazotrophs in the ocean, Biogeosciences, 4, 31–57, 2007.

Orcutt, K. M., Lipschultz, F., Gundersen, K., Arimoto, R., Michaels, A. F., Knap, A. H. and Gallon, J. R.: A seasonal study of the significance of N_2 fixation by *Trichodesmium* spp. at the Bermuda Atlantic Time-series Study (BATS) site, Deep-Sea Res. II, 48, 1583–1608, 2001.

Pahlow, M. and Riebesell, U.: Temporal Trends in Deep Ocean Redfield Ratios, Science, 287, 831–833, doi:10.1126/science.287.5454.831, 2000.

Price, N. M.: The elemental stoichiometry and composition of an iron-limited diatom, Limnol. Oceanogr., 50(4), 1159–1171, 2005.

Quigg, A., Finkel, Z. V., Irwin, A. J., Rosenthal, Y., Ho, T.-Y., Reinfelder, J. R., Schofield, O., Morel, F. M. M. and Falkowski, P. G.: The evolutionary inheritance of elemental stoichiometry in marine phytoplankton, Nature, 425, 291–294, 2003.

Redfield, A. C.: On the proportions of organic derivatives in seawater and their relation to the composition of plankton, in James Johnstone Memorial Volume, pp. 176–192, university press of liverpool, Liverpool, UK., 1934.

Redfield, A. C.: The biological control of chemical factors in the environment, Am. Sci., 46, 205–221, 1958.

Rhee, G.-Y.: Effects of N:P atomic ratios and nitrate limitation on algal growth, cell composition, and nitrate uptake, Limnol. Oceanogr., 23(1), 10–25, 1978.

Roussenov, V. M., Williams, R. G., Mahaffey, C. and Wolff, G. A.: Does the transport of dissolved organic nutrients affect export production in the Atlantic Ocean?, Glob. Biogeochem. Cycles, 20(GB3002), doi:10.1029/2005GB002510, 2006.

Salihoglu, B., Garcon, V., Oschlies, A., Lomas, M.W. 2007. Influence of nutrient remineralization and utilization stoichiometry on phytoplankton species and carbon export: A modeling study at BATS. Deep Sea Res. I, 55: 73-107.

Sañudo-Wilhelmy, S. A., Kustka, A. B., Gobler, C. J., Hutchins, D. A., Yang, M., Lwiza, K., Burns, J., Capone, D. G., Raven, J. A. and Carpenter, E. J.: Phosphorus limitation of nitrogen fixation by *Trichodesmium* in the central Atlantic Ocean, Nature, 411, 66–69, 2001.

556 Sañudo-Wilhelmy, S. A., Tovar-Sanchez, A., Fu, F.-X., Capone, D. G. and Hutchins, D. A.: The
557 impact of surface-adsorbed phosphorus on phytoplankton Redfield stoichiometry, Nature, 432,
558 897–901, 2004.

559 Schaefer, K., Denning, A. S. and Leonard, O.: The winter Arctic Oscillation, the timing of
560 spring, and carbon fluxes in the Northern Hemisphere, Glob. Biogeochem. Cycles, 19, GB3017,
561 doi:10.1029/2004GB002336, 2005.

562 Siegel, D. A., Westberry, T. K., O'Brien, M. C., Nelson, N. B., Michaels, A. F., Morrison, J. R.,
563 Schott, A., Caporelli, E. A., Sorenson, J. C., Maritorena, S., Garver, S. A., Brody, E. A., Ubante,
564 J. and Hammer, M. A.: Bio-optical modeling of primary production on regional scales: the
565 Bermuda BioOptics project, Deep-Sea Res. II, 48, 1865–1896, 2001.

566 Sigman, D. M. and Boyle, E. A.: Glacial/interglacial variations in atmospheric carbon dioxide,
567 Nature, 407, 859–869, 2000.

568 Singh, A., Lomas, M. W. and Bates, N. R.: Revisiting N_2 fixation in the North Atlantic Ocean:
569 significance of deviations in Redfield Ratio, atmospheric deposition and climate variability,
570 Deep-Sea Res. II, 93, 148–158, doi:10.1016/j.dsr2.2013.04.008, 2013.

571 Steinberg, D. K., Carlson, C. A., Bates, N. R., Johnson, R. J., Michaels, A. F. and Knap, A. H.:
572 Overview of the US JGOFS Bermuda Atlantic Time-series Study (BATS): a decade-scale look at
573 ocean biology and biogeochemistry, Deep-Sea Res. II, 48, 1405–1447, 2001.

574 Teng, Y.-C., Primeau, F. W., Moore, J. K., Lomas, M. W. and Martiny, A. C.: Global-scale
575 variations of the ratios of carbon to phosphorus in exported marine organic matter, Nat. Geosci.,
576 7, 895–898, doi:10.1038/NGEO2303, 2014.

577 Thompson, D. W. J. and Wallace, J. M.: The Arctic Oscillation signature in wintertime
578 geopotential height and temperature fields, Geophys. Res. Lett., 25(9), 1297–1300, 1999.

579 Torres-Valdés, S., Roussenov, V. M., Sanders, R., Reynolds, S., Pan, X., Mather, R., Landolfi,
580 A., Woff, G. A., Achterberg, E. P. and Williams, R. G.: Distribution of dissolved organic
581 nutrients and their effect on export production over the Atlantic Ocean, Glob. Biogeochem.
582 Cycles, 23, GB4019, doi:10.1029/2008GB003389, 2009.

583 Tyrrell, T.: The relative influences of nitrogen and phosphorus on oceanic primary production,
584 Nature, 400, 525–531, 1999.

585 Vidal, M., Durate, C. M. and Agustí, S.: Dissolved organic nitrogen and phosphorus pools and
586 fluxes in the central Atlantic Ocean, Limnol. Oceanogr., 44(1), 106–115, 1999.

587 Voss, M. and Hietanen, S.: The depths of nitrogen cycling, Nature, 493, 616–618, 2013.

588 Weber, T. S. and Deutsch, C. A.: Ocean nutrient ratios governed by plankton biogeography,
589 Nature, 467, 550–554, doi:10.1038/nature09403, 2010.

590 Williams, R. G. and Follows, M. J.: The Ekman transfer of nutrients and maintenance of new
591 production over the North Atlantic, Deep-Sea Res. I, 45, 461–489, 1998.

592 Wu, J., Sunda, W., Boyle, E. A. and Karl, D. M.: Phosphate Depletion in the Western North
593 Atlantic Ocean, Science, 289, 759–762, doi:10.1126/science.289.5480.759, 2000.

594 Zamora, L. M., Landolfi, A., Oschlies, A., Hansell, D. A., Dietze, H. and Dentener, F.:
595 Atmospheric deposition of nutrients and excess N formation in the North Atlantic,
596 Biogeosciences, 7, 777–793, 2010.

597

598

599

600

601

602

603 **Table 1.** Average concentration (μmol kg^{-1}), molar ratio of various biogeochemical parameters

604 and particle fluxes (mmol m^2 d^{-1}) from the BATS data presented in Fig. 1.

Concentration (C) in the upper 100 m			
Parameter	C ± σ*	no of samples	Sampling period
TOC	63.81 ± 2.86	714	Jan 2004 - Dec 2011
TON	4.43 ± 0.50	712	Jan 2004 - Dec 2011
TOP	0.07 ± 0.03	547	Jun 2004 - Nov 2011
POC	2.36 ± 1.14	844	Jan 2004 - April 2012
PON	0.40 ± 0.19	845	Jan 2004 - April 2012
POP	0.01 ± 0.01	696	Jan 2004 - April 2012
Ratio (R)† in the upper 100 m			
Parameter	R ± σ	no of data points€	Sampling period
TOC:TON	15 ± 0.5	86	Jul 2004 - Dec 2011
POC:PON	6 ± 3	95	Jan 2004 - Apr 2012
TON:TOP	68 ± 9	77	Jul 2004 - Nov 2011
PON:POP	36 ± 11	88	Jan 2004 - Apr 2012
TOC:TOP	983 ± 168	78	Jul 2004 - Nov 2011
POC:POP	210 ± 67	88	Jan 2004 - Apr 2012
Inorganic nutrient stoichiometry in 100-500 m			
Parameter	(C or R) ± σ	no of data points	Sampling period
NO_3^-	2.74 ± 2.40	3425	Oct 1988 - July 2012
PO_4^{3-}	0.11 ± 0.13	3405	Oct 1988 - July 2012
NO_3^-:PO_4^{3-}	25.6 ± 9.1	2415	Oct 1988 - July 2012
Particle fluxes at 200 m			
Parameter	C ± σ	no of samples	Sampling period
C	1.68 ± 1.07	254	Jan 1989 - Dec 2011
N	0.23 ± 0.16	254	Jan 1989 - Dec 2011
P	0.008 ± 0.014	64	Oct 2005 - Dec 2011
Ratio in particle fluxes at 200 m			
Parameter	R ± σ	no of data points	Sampling period
N:P	57 ± 46	61	Oct 2005 - Dec 2011
C:P	287 ± 269	62	Oct 2005 - Dec 2011
C:N	7.9 ± 2.8	252	Jan 1989 - Dec 2011

605 *σ is standard deviation of the samples mentioned in next the column. †Ratios and their standard
606 deviations are derived from the monthly mean values (€one datum would be mean of many
607 values of concentration for a particular month) of concentration in the upper 100 m.
608
609
610
611

Figure Captions:

Fig. 1. Monthly BATS data on C, N and P in total and particulate organic matter in top 100 m during Jan 2004 to April 2012.

Fig. 2. Monthly stoichiometry during 2004-2010 at 0-100 m. Solid lines are three month running means. Error bars are 1σ standard deviations from the mean values.

Fig. 3. Mixed layer depth (MLD) during the sampling period at BATS site.

Fig. 4. Box/whisker plot comparing the annual concentrations of total (open bars) and particulate organic matter (filled bars) relative to the deep mixing in 0-25 m depth at BATS (data used from January 2005 - December 2011). Bottom and top of the box define the 25% and 75% data distribution, and the 'error' bars define the 5% and 95% data distribution. The dark gray vertical bar represents the period of deep mixing (DM) for each year.

Fig. 5. Box/whisker plot comparing the annual concentrations of total (open bars) and particulate (filled bars) matter relative to the deep mixing at 25-100 m depth (data used from January 2005 - December 2011). All else as in Figure 4.

Fig. 6. Box/whisker plot comparing the annual ratios of elemental stoichiometry relative to the deep mixing at 0-25 m depth (data used from January 2005 - December 2011). All else as in Figure 4.

Fig. 7. Box/whisker plot comparing the annual ratios of elemental stoichiometry relative to the deep mixing at 25-100 m depth (data used from January 2005 - December 2011). The gray bar represents the period of deep mixing (DM) for each year. All else as in Figure 4.

Fig. 8. Box/whisker plot comparing the annual variation of NO_3^- and PO_4^{3-} and their ratio relative to the deep mixing at 100-500 m depth (data used from January 2005 - December 2011). The gray bar represents the period of deep mixing (DM) for each year. All else as in Figure 4.

Fig. 9. Box/whisker plot comparing the annual variation in Chlorophyll *a* and cell counts for *Prochlorococcus*, *Synechococcus*, Picoeukaryotes, and Nanoeukaryotes relative to the deep mixing in 0-25 m depth at BATS (data used from January 2005 - December 2011). The gray bar represents the period of deep mixing for each year. All else as in Figure 4.

Fig. 10. Relationship between TOP (Dec 2006 - Jan 2008) and (a) cell abundances (natural log transformed) of *Prochlorococcus*, *Synechococcus,* Picoeukaryotes and Nanoeukaryotes during Sep 2006 - Nov 2007. Among cell abundances, only Nanoeukaryotes showed a significant relationship with TOP (r^2 = 0.61, p < 0.001) (b) Relationship between TOP and Arctic Oscillation index during Nov 2005 - Dec 2006 (r^2 = 0.46, p < 0.01).

Fig.1

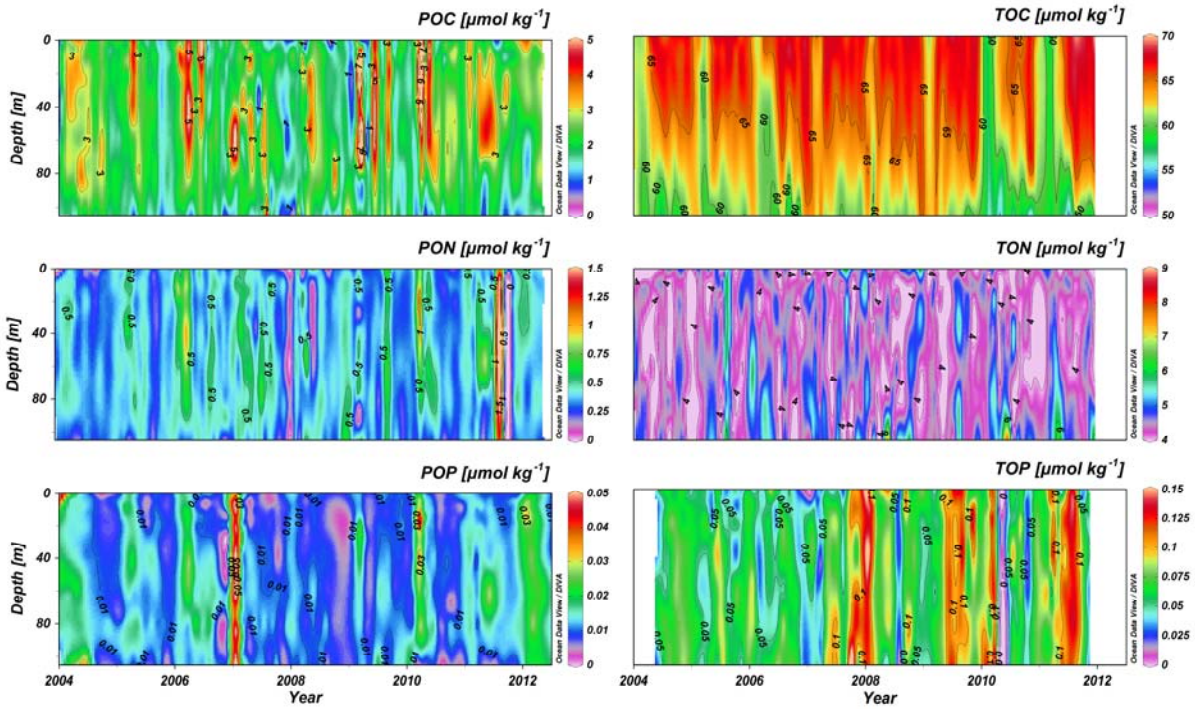
POC [μmol kg-1]
TOC [μmol kg-1]
PON [μmol kg-1]
TON [μmol kg-1]
POP [μmol kg-1]
TOP [μmol kg-1]
Depth [m]
Year
2004
2006
2008
2010
2012
Ocean Data View / DIVA

673 **Fig. 2**

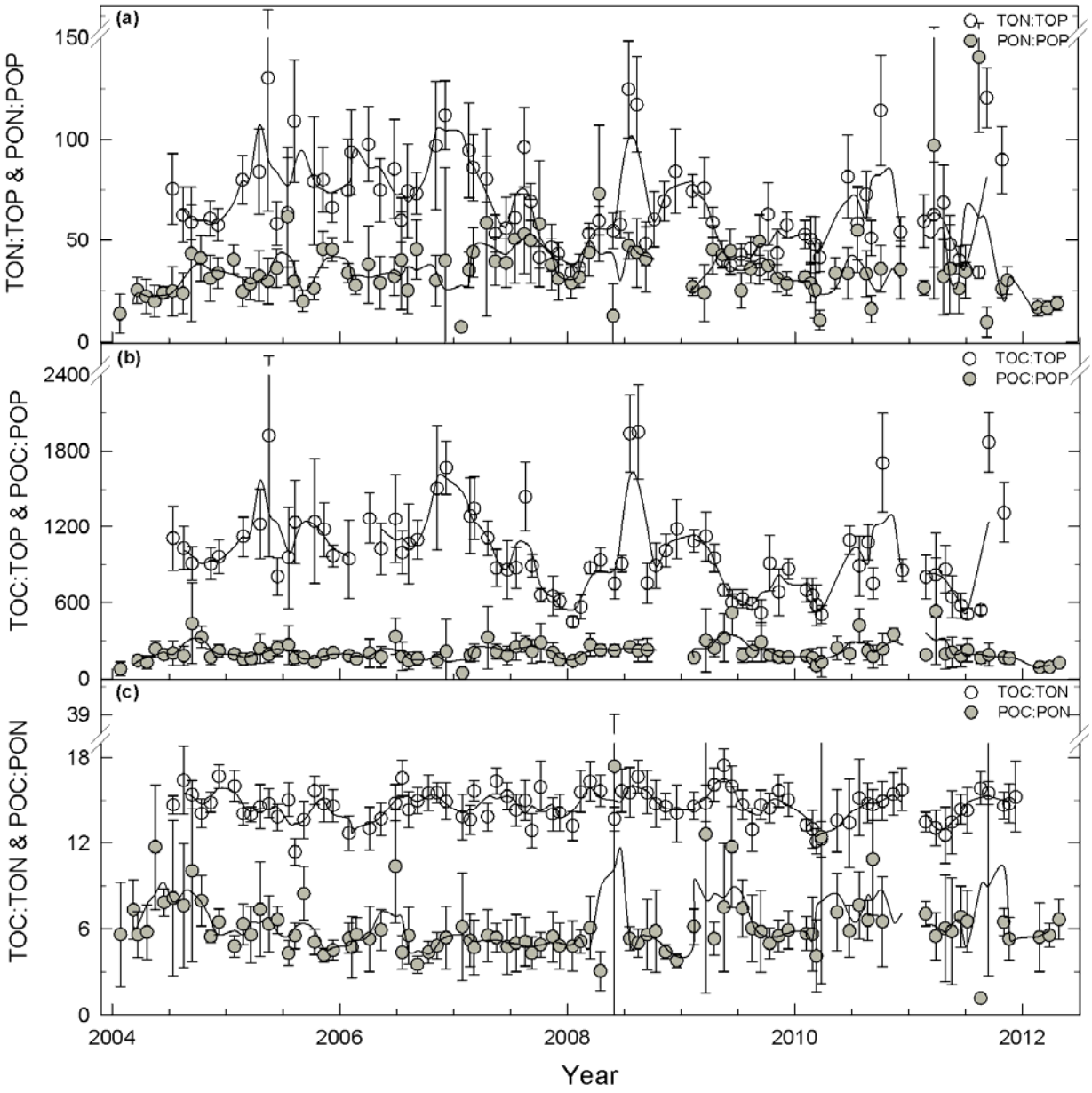

674

675

676

677

678

679

Fig. 3

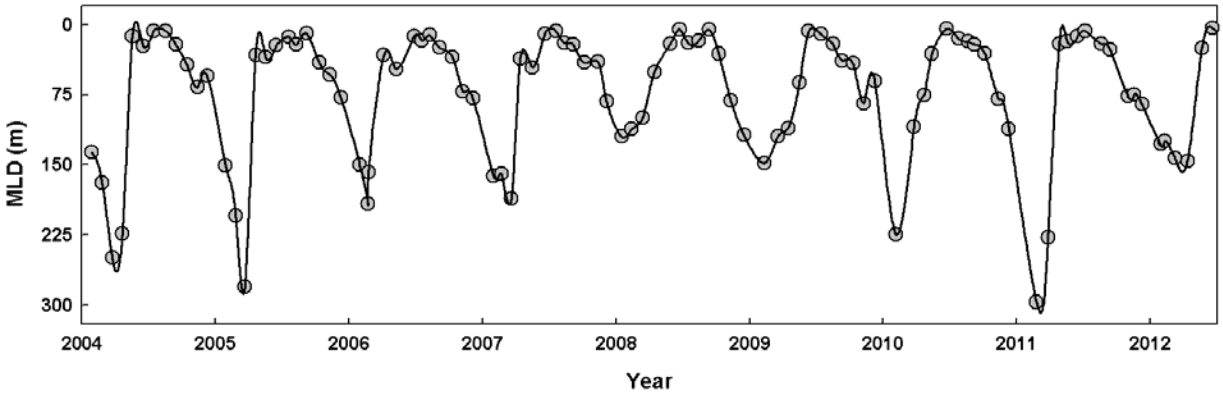
MLD (m)
0
75
150
225
300
2004
2005
2006
2007
2008
2009
2010
2011
2012
Year

Fig. 4

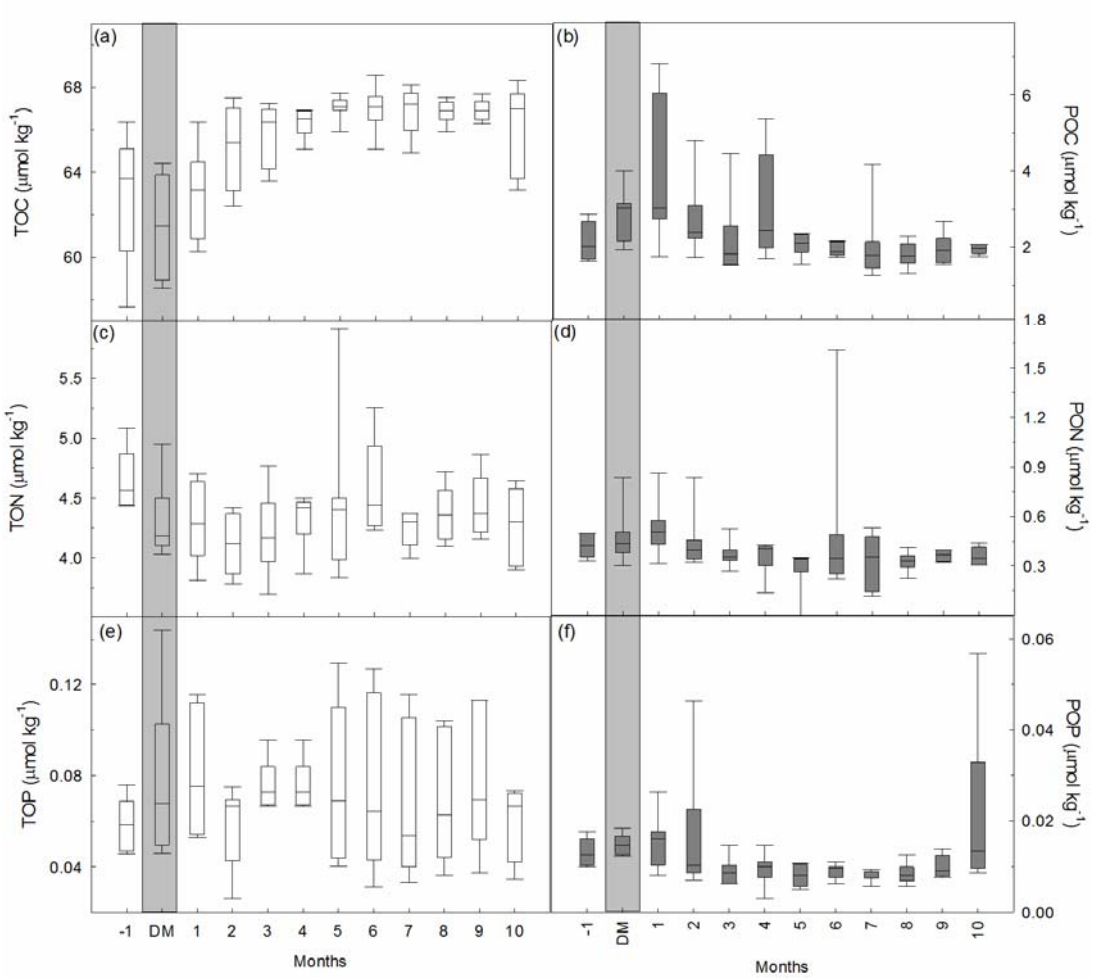
(a)
(b)
(c)
(d)
(e)
(f)
TOC (µmol kg-1)
POC (µmol kg-1)
TON (µmol kg-1)
PON (µmol kg-1)
TOP (µmol kg-1)
POP (µmol kg-1)
-1
DM
1
2
3
4
5
6
7
8
9
10
Months

704 **Fig. 5**

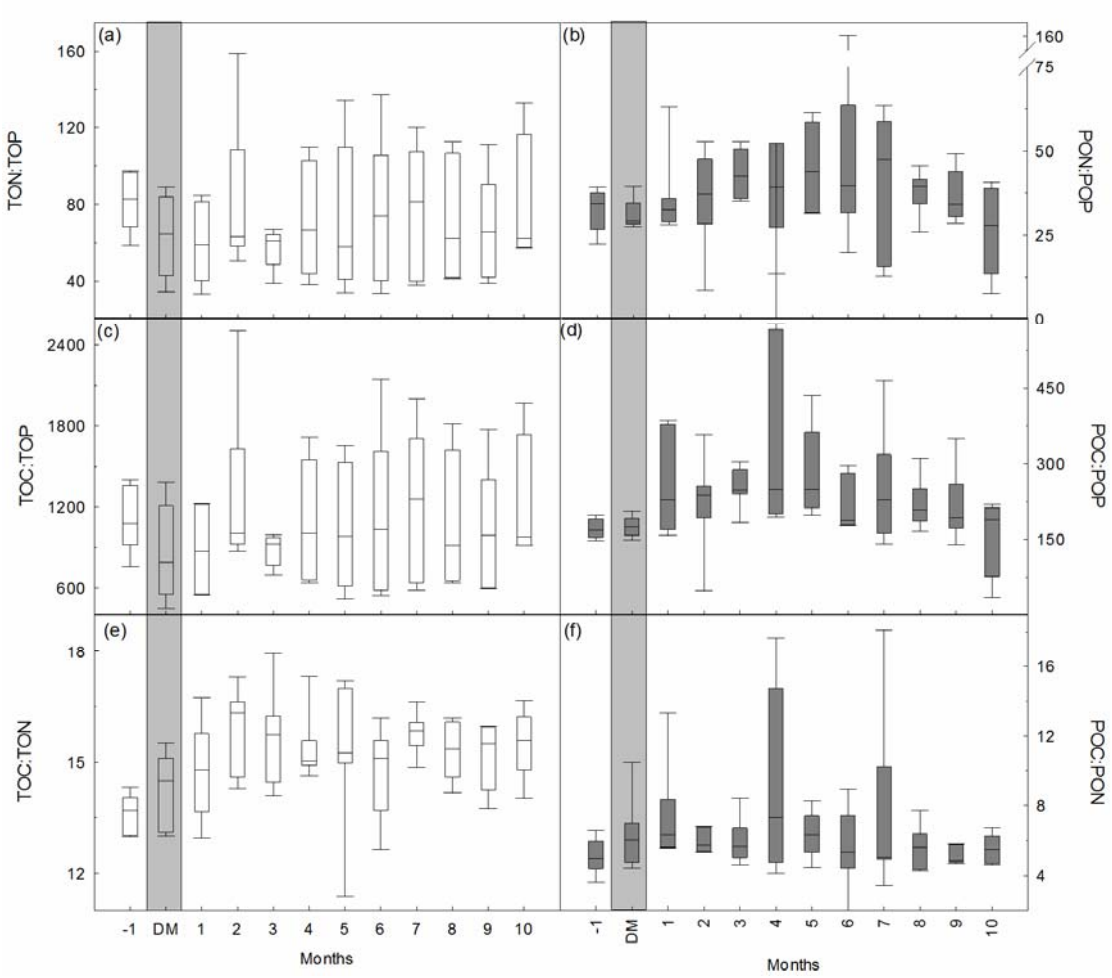

705

706

707

708

709

710 **Fig. 6**

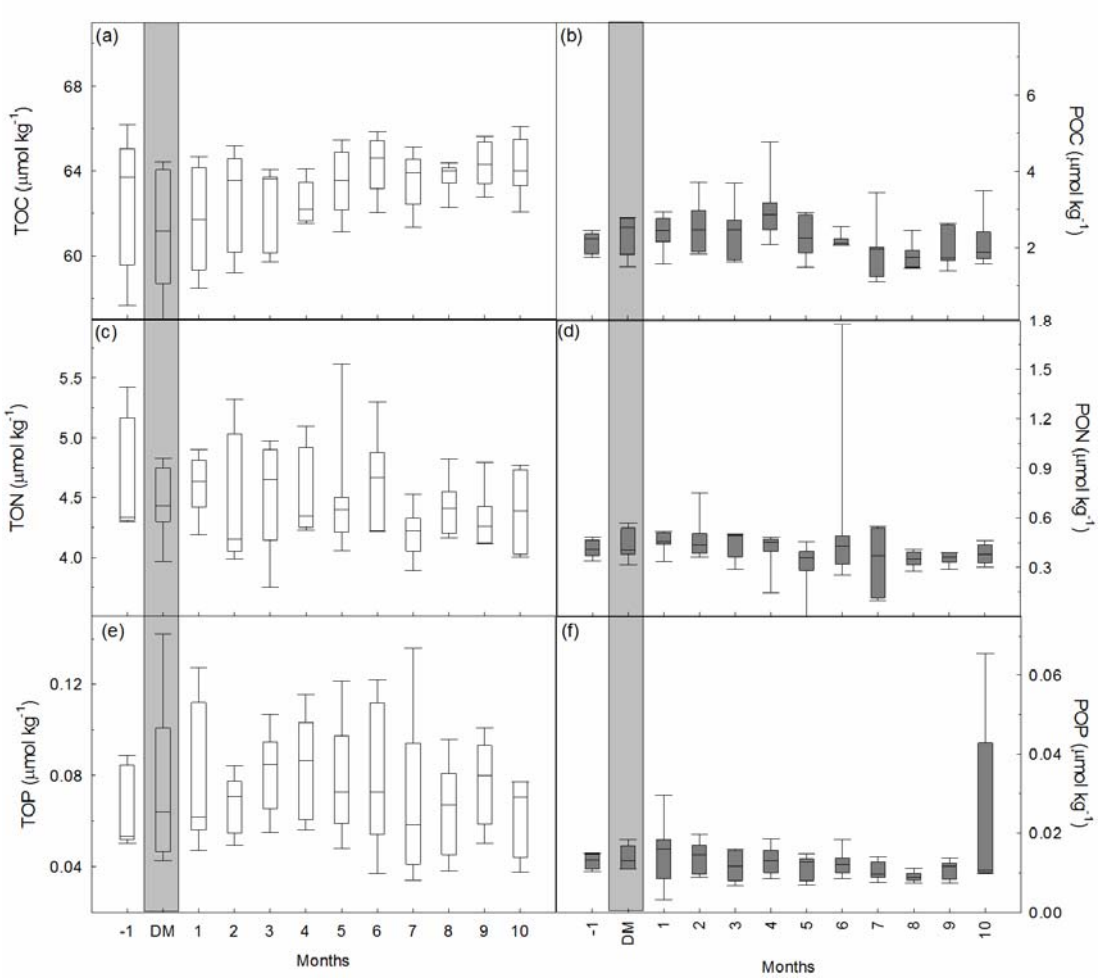

711

712

713

714

715

716 **Fig. 7**

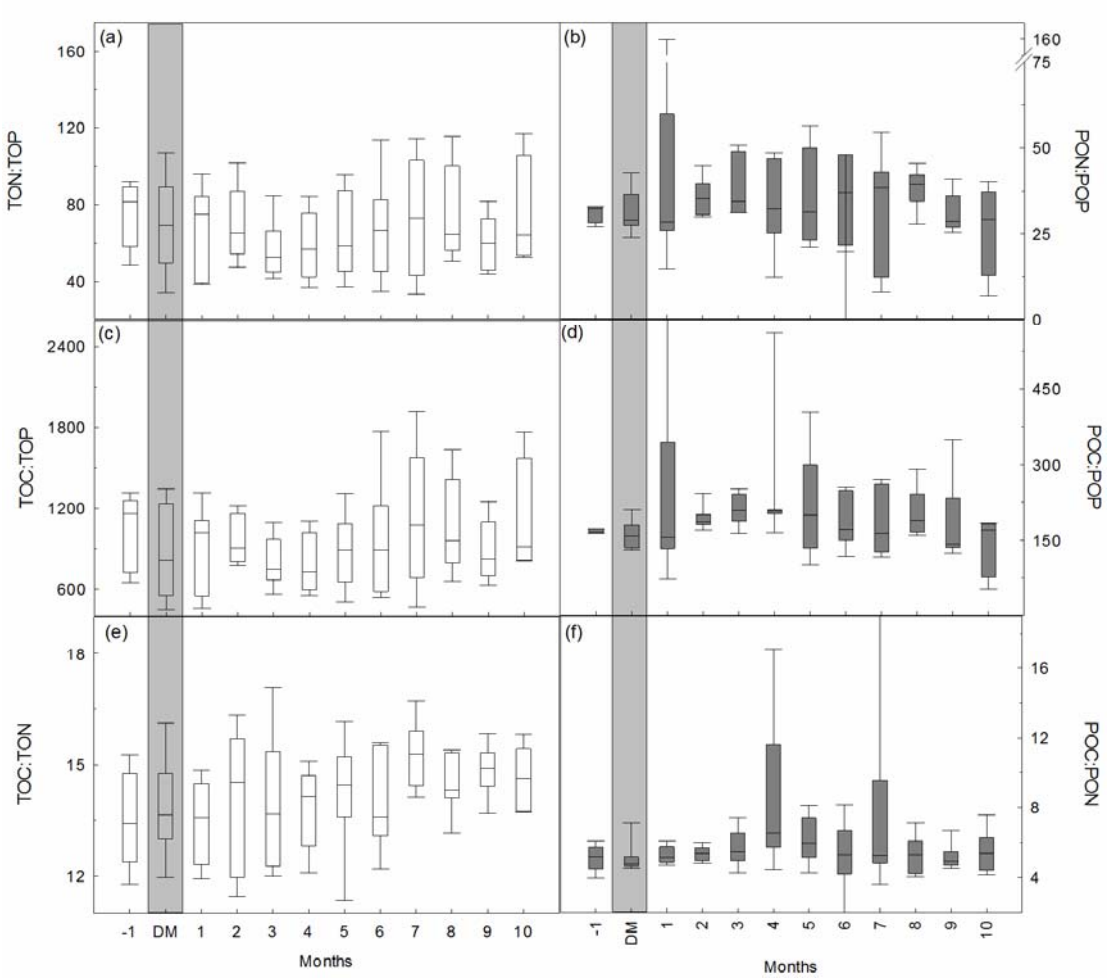

717

718

719

720

721

722 **Fig. 8**

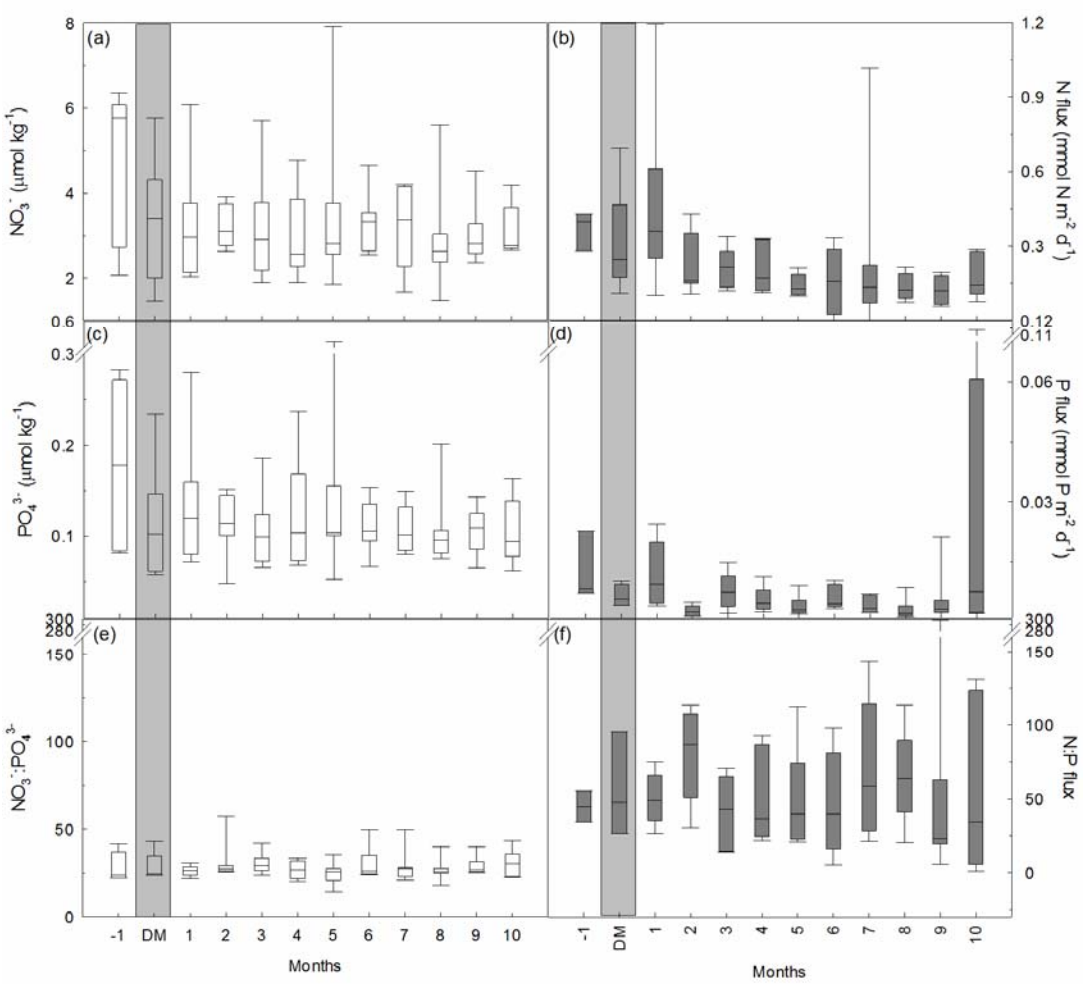

723

724

725

726

727 **Fig. 9**

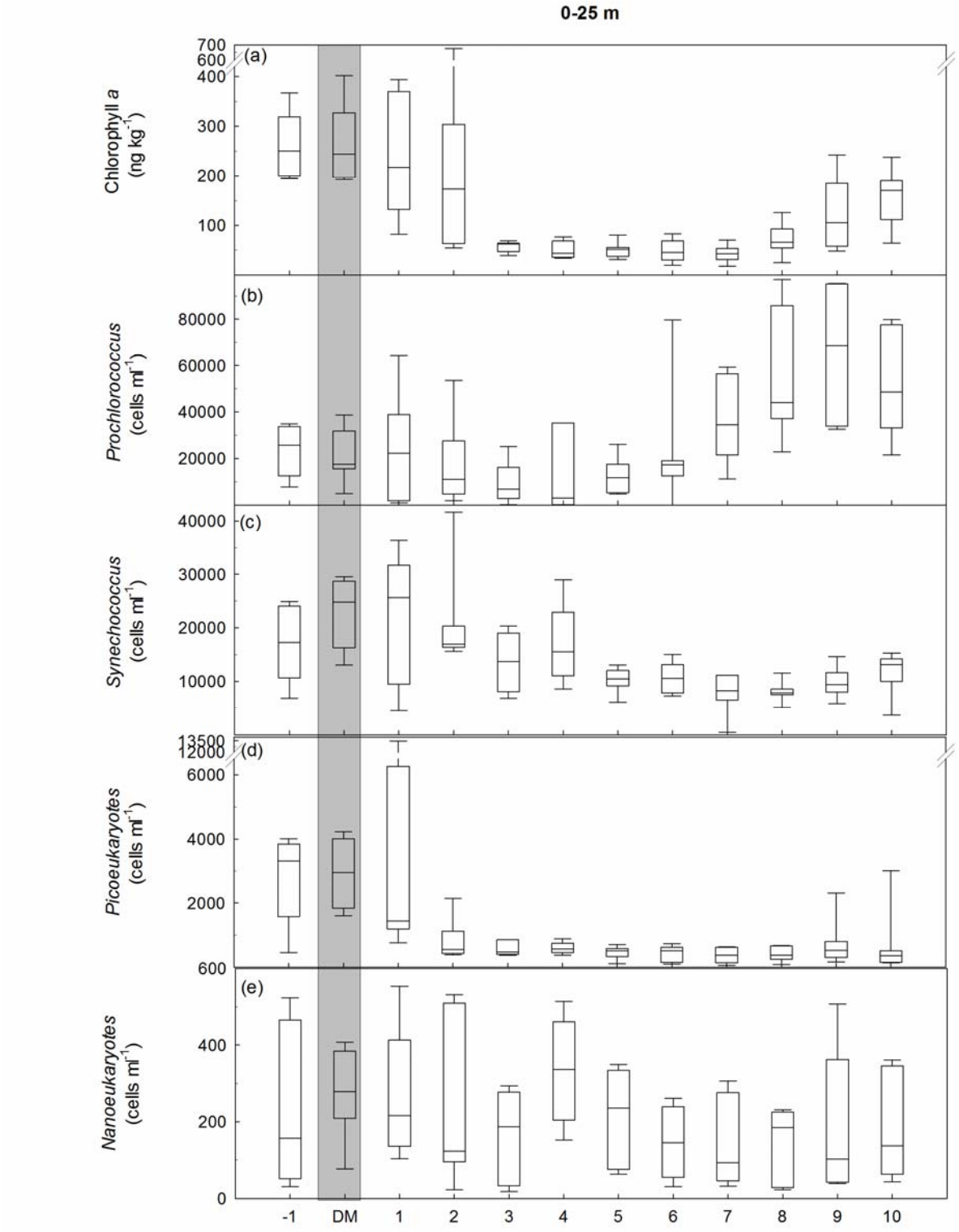

728

729

730 **Fig. 10**

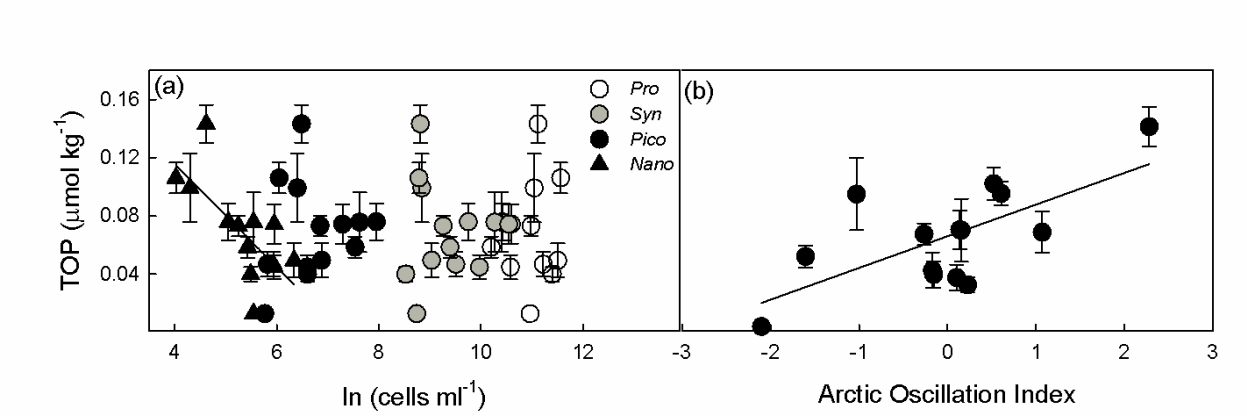

731

732

733